JGR Atmospheres

RESEARCH ARTICLE
10.1029/2019JD031909

Special Section:
Atmospheric PM2.5 in China: physics, chemistry, measurements, and modeling

Key Points:
- We provide a first insight into characterization of aerosol type over East Asia with 4.4 km MISR products
- Obvious improvements are found in MISR AOD with large potential in inferring aerosol types
- MISR retrievals are sensitive to aerosol microphysical properties but with different reliabilities

Supporting Information:
- Supporting Information S1

Correspondence to:
M. Tao and L. Chen,
taomh@cug.edu.cn;
chenlf@radi.ac.cn

Citation:
Tao, M., Wang, J., Li, R., Chen, L., Xu, X., Wang, L., et al. (2020). Characterization of aerosol type over East Asia by 4.4 km MISR product: First insight and general performance. *Journal of Geophysical Research: Atmospheres*, *125*, e2019JD031909. https://doi.org/10.1029/2019JD031909

Received 27 OCT 2019
Accepted 29 APR 2020
Accepted article online 1 JUN 2020

Author Contributions:
Conceptualization: Minghui Tao
Formal analysis: Minghui Tao
Investigation: Rong Li
Methodology: Minghui Tao, Rong Li, Xiaoguang Xu, Zifeng Wang
Resources: Liangfu Chen, Lunche Wang, Jinhua Tao
Validation: Rong Li, Juan Xiang
Visualization: Minghui Tao, Rong Li
Writing - original draft: Minghui Tao
Writing – review & editing: Jun Wang, Liangfu Chen, Xiaoguang Xu

Characterization of Aerosol Type Over East Asia by 4.4 km MISR Product: First Insight and General Performance

Minghui Tao[1], Jun Wang[2], Rong Li[3], Liangfu Chen[4], Xiaoguang Xu[5], Lunche Wang[1], Jinhua Tao[4], Zifeng Wang[4], and Juan Xiang[1]

[1]Hubei Key Laboratory of Critical Zone Evolution, School of Geography and Information Engineering, China University of Geosciences, Wuhan, China, [2]Department of Chemical and Environmental Engineering, University of Iowa, Iowa City, IA, USA, [3]School of Resources and Environmental Science, Hubei University, Wuhan, China, [4]State Key Laboratory of Remote Sensing Science, Aerospace Information Research Institute, Chinese Academy of Sciences, Beijing, China, [5]Joint Center for Earth Systems and Technology, University of Maryland, Baltimore County, Baltimore, MD, USA

Abstract The lack of aerosol type information has largely hindered satellite products from further applications such as constraining model simulations and quantifying aerosol climate effects. The recent Version (V) 23 Multi-angle Imaging Spectroradiometer (MISR) aerosol products with an enhanced spatial resolution at 4.4 km enable an unprecedented chance to explore aerosol types and associated processes in the regional scale. Here we provide a comprehensive insight into the characterization of MISR aerosol optical and microphysical properties, as well as their performance, over East Asia. Ground validation shows a remarkable improvement in the accuracy of V23 MISR aerosol optical depth (AOD) with ~80% of its retrieval bias within $\pm(0.05 + 20\%\mathrm{AOD}_{\mathrm{AERONET}})$. However, an underestimation of MISR AOD is still prevalent in the high-AOD (>0.6) conditions, due to the surface-atmosphere separation problem and insufficient absorbing aerosol mixtures being selected. MISR AOD of different size bins agrees well with AErosol RObotic NETwork (AERONET) results, demonstrating an evident advantage in discriminating natural dust from anthropogenic particles. Although MISR nonspherical and absorbing retrievals display a consistent variation with the AERONET inversions, their component AODs have a poor reliability over East Asia due to the inappropriate aerosol component models or their mixtures as in V22. In particular, the most striking problem is the sparse and discrete MISR absorbing retrievals with spatial discontinuity. Generally, the high-resolution V23 MISR products exhibit a great potential in characterizing the regional variations of aerosol type, which can be further refined by considering the prior aerosol knowledge over East Asia.

1. Introduction

Atmospheric aerosol is a complex mixture of particles with different sizes, shapes, and chemical components, originating from diverse emission sources and subject to dynamic meteorological cycles. These tiny particles have exerted intensive and intricate influences on the Earth's climate system by modifying the distribution of solar radiance (Christian et al., 2019; Ge et al., 2016; Koren et al., 2004; Li et al., 2017; Wang et al., 2013), the properties of cloud (Chen et al., 2016; Wang et al., 2015), and precipitation (Fan et al., 2012; Guo et al., 2016; Liu et al., 2020), which can be generally attributed to aerosol-radiation interaction and aerosol-cloud interaction effects (Boucher et al., 2013; Li et al., 2019). Besides, numerous epidemiological studies have shown a robust correlation between inhalation levels of ambient fine particles ($PM_{2.5}$) and adverse health effects such as increased chronic respiratory and cardiovascular diseases (Pope et al., 2002). However, the amount and properties of atmospheric aerosols have a large variability over space and time due to their short lifetime spanning from a few hours to several days, diverse emission sources, and complicated secondary formation processes. So far, accurate quantification of aerosol properties with sufficient spatial and temporal resolution remains a challenge in associated climate and air quality researches.

Considering the necessity of aerosol observations from regional to global scales, a series of dedicated satellite instruments such as Moderate Resolution Imaging Spectroradiometer (MODIS), Multi-angle Imaging Spectroradiometer (MISR), and Polarization and Directionality of the Earth's Reflectances (POLDER) have been launched since the late 1990s (King et al., 1999). The emerging satellite aerosol products over land have greatly advanced our knowledge regarding variations of global aerosol loading and major sources (Kaufman et al., 2002). Moreover, by taking advantage of integrated spectral, angular, or polarimetry measurements, satellite sensors such as MISR and POLDER can obtain abundant aerosol optical and microphysical properties concerning particle size and components (Dubovik et al., 2019) and, to some degree, the aerosol vertical distribution (Ding et al., 2016; Xu et al., 2019). In addition to aerosol amount, quantitative information of aerosol type is crucial in validating and constraining numerical climate and chemistry models (Lee et al., 2016; Li et al., 2013) and to improve the emission estimates of aerosols (Chen et al., 2018; Wang et al., 2012) and the monitoring of surface $PM_{2.5}$ concentration (Liu et al., 2007; Meng et al., 2018). However, those sophisticated satellite sensors usually have a narrow swath width or coarse spatial resolution, and validation of their aerosol type products is challenging due to the lack of ground measurements with robust accuracy (Kahn & Gaitley, 2015). As a result, the most commonly used satellite aerosol parameter over land is still the aerosol optical depths (AODs), such as those from the multispectral MODIS retrieval with a daily near-global coverage.

The MISR instrument on board Terra satellite has provided continuous global observations in four visible/near-infrared spectral bands from nine viewing angles since 2000 (Kahn et al., 2001). The unique multiangle measurements of MISR contain valuable information regarding aerosol microphysical properties such as particle size and shape (Diner et al., 2005; Kahn et al., 1998), which can be used to infer aerosol components (Kahn & Gaitley, 2015; Liu et al., 2007). However, MISR aerosol products have limited applications, especially in the regional scales, due largely to the coarse resolution (~17.6 km) in the Version (V) 22 and the narrow swath width (~380 km). Recently, the new V23 MISR aerosol products has been upgraded with a much finer resolution of 4.4 km along with the enhanced accuracy and coverage (Garay et al., 2017, 2020), enabling an important opportunity to map aerosol components from space. In addition, the operational MISR products can be a ready-made platform to examine retrieval potential of angular information for future multiangle polarimetric sensors such as the Multi-Angle Imager for Aerosols (MAIA) instrument (Diner et al., 2018).

In this study, we provide a comprehensive view on the characterization of aerosol type over East Asia with the V23 high-resolution MISR products as well as their performance. The main purpose of this work is to give a reference for the potential of satellite multiangle measurements for the aerosol retrievals and their associated applications over East Asia, an area with frequently high aerosol loading and diverse emission sources. Section 2 gives a brief introduction of the V23 MISR aerosol products as well as ground-based measurements used for validation. Performance of MISR retrievals in characterizing aerosol optical properties and component information in different surface types is shown and evaluated in detail in sections 3.1 and 3.2. In addition, uncertainties and implications of MISR multiangle retrievals are discussed in section 3.3. Section 4 summarizes our findings and primary conclusions.

2. Data and Methods

2.1. MISR Aerosol Data Sets

MISR instrument carries nine same cameras to image the Earth at nine different view angles (0° at nadir and ±26.1°, ±45.6°, ±60.0°, and ±70.5° forward or backward of the direction of satellite motion), enabling observations at a large range of scattering angles within ~60–160° (Diner et al., 2005). These MISR cameras have four visible/near-infrared spectral bands (446, 558, 672, and 866 nm) and high spatial resolution at 275 m or 1.1 km that makes aerosol retrievals insusceptible to clouds. However, the narrow swath width of ~380 km leads to the global coverage of MISR with a 9 day cycle. To infer aerosol types with MISR's combined multispectral and multiangle information, 74 aerosol mixtures defined by particle size, shape, complex refractive index, and scale height are used to represent the variations of actual aerosol properties (Liu et al., 2007; Martonchik et al., 2009). These 74 mixtures are divided into three groups: spherical nonabsorbing (1–30), spherical absorbing and nonabsorbing mixture (41–50), and nonspherical dust components (51–74). Each mixture is assumed to be composed of two or three from eight "pure" particle components with each characterized by a single size distribution and specific optical properties (Kahn & Gaitley, 2015).

MISR aerosol retrieval searches the best match between observed top of the atmosphere (TOA) radiances and simulated counterparts in look-up tables (LUT) precalculated with those 74 aerosol mixtures for different AOD values at different geometries. The spherical nonabsorbing mixtures (1–30) is a combination of three fine-mode components with effective radius (r_{eff}) of 0.06, 0.12, and 0.26 μm and a coarse-mode component (2.8 μm), respectively, which mainly represent water-soluble particles such as sulfate (Liu et al., 2007).

The spherical absorbing mixture (31–50) includes two absorbing spherical components with single scattering albedo (SSA, 0.8 or 0.9 at green band) mixed with the same coarse-mode component in the nonabsorbing mixtures. The mixtures of 51–74 are two nonspherical dust components with medium and large sizes and their mixing with two nonabsorbing components ($r_{\mathrm{eff}} = 0.12$ and 2.8 μm). A summary of the retrieved MISR aerosol components is given as small, medium, and large size bins, with specific particle radii <0.35, 0.35–0.7, and >0.7 μm, respectively (Kahn et al., 2010).

With the same retrieval principle as V22 except some slight refinements such as cloud screening, the V23 MISR algorithm provides aerosol products at a much higher spatial resolution of 4.4 km (Garay et al., 2020). Global assessments of V22 MISR AOD and its aerosol type products have identified a number of typical issues in MISR retrievals (Kahn et al., 2010; Kahn & Gaitley, 2015). It is suggested that there is a general lack of particle component models with specific sizes and their mixtures, which would cause AOD bias and hamper the discrimination of aerosol type. Owing to the lack of appropriate absorbing particles, V22 MISR products systematically overestimate the SSA (<1.0) values. Moreover, MISR AOD underestimation tends to occur frequently for an AErosol RObotic NETwork (AERONET) AOD > 0.4. It is speculated that in high-AOD conditions, AOD variability within the V22's 17.6 km retrieval region could be in part assigned to the surface and becomes a leading factor in the AOD underestimation when SSA is near or at 1.0 (Kahn et al., 2010). For absorbing particles, the nonabsorbing mixtures mostly selected in MISR retrievals can also contribute to the AOD underestimation. Additionally, the sensitivity of MISR retrievals to aerosol type diminishes obviously for AODs below 0.15 or 0.2.

2.2. AERONET Measurements

AERONET is a ground-based remote sensing network of Sun photometers that measure aerosol properties from direct sunlight and scattered sky light since the 1990s (Holben et al., 1998). Direct Sun observations provide the columnar spectral AOD at a very high accuracy (~0.01–0.02) every 5 to 15 min in cloud-free conditions (Eck et al., 1999), which is usually considered as "ground truth" in the evaluation of satellite retrievals. By using the combined direct sunlight and sky light measurements, AERONET also delivers inversion products for aerosol size distribution, complex refractive index, and nonsphericity with a reliable accuracy (Dubovik, Holben, Eck, et al., 2002). Sensitivity simulations showed that errors of AERONET size distribution do not exceed 10% of the maxima in 0.1–7 μm range (Dubovik & King, 2000). Only being retrieved for $\mathrm{AOD}_{440} > 0.4$ and solar zenith angles >50°, AERONET complex refractive indices are retrieved with errors within ~30–50% for the imaginary part and 0.04 for the real part. For nonsphericity, ~90% of AERONET dust retrievals (>3,000 cases) in desert sites exhibited significant improvements when nonspherical shape was considered (Dubovik, Holben, Lapyonok, et al., 2002).

Previous validations of MISR products mainly focused on AOD (Christopher & Wang, 2004; Kahn et al., 2010; Liu et al., 2010), and a global analysis by Kahn and Gaitley (2015) gave a regional assessment of V22 MISR aerosol type products in eastern China during January and July 2007. With the long-term V23 MISR products during 2001–2018, we extend these previous studies to make a detailed assessment of the performance of these high-resolution MISR retrievals for both AOD and aerosol types with AERONET inversions in typical regions of East Asia. Our validation uses the recent Version 3 Level (L) 2.0 AERONET AOD and inversion products, which have improved data processing and instrument calibration (Giles et al., 2019). Figure 1 shows locations of the nine selected AERONET sites in typical surface types. Considering the low temporal resolution of MISR observations, only AERONET sites with more than 3 years of continuous observations are selected. Consistent with previous studies (Garay et al., 2017), our validation compares the spatial averages of instantaneous MISR aerosol retrievals within a radius of ~25 km around AERONET sites with the temporal mean of AERONET observations within 1 hr of MISR's passing time (Ichoku et al., 2002). AERONET spectral AODs at 440 and 675 nm are interpolated to match with MISR AOD at 550 nm.

For aerosol type, we evaluate MISR retrievals of small- and large-mode AODs by comparing with AERONET fine- and coarse-mode AODs from the spectral deconvolution algorithm (SDA), respectively. It should be noted that there are different definitions of those aerosol modes between AERONET and MISR. While the dynamic separation points for AERONET fine and coarse modes range from 0.439 to 0.992 μm (https://aeronet.gsfc.nasa.gov/new_web/optical_properties.html), MISR retrieval algorithm uses fixed radius intervals of <0.3 and >0.7 μm for small and large aerosol modes. MISR and AERONET SSA at 446 and 440 nm is compared directly. Since nonsphericity parameter is not available in the V3 L2 AERONET inversions, we take

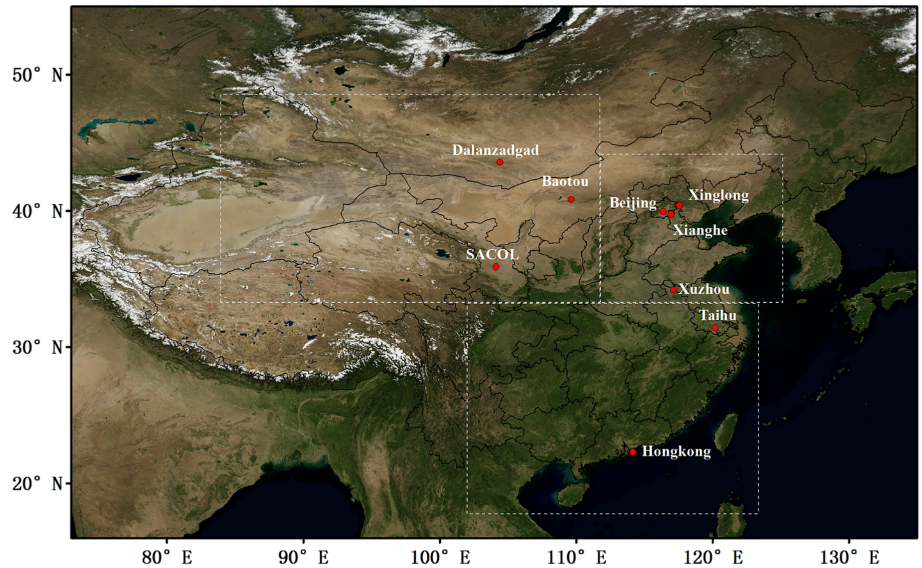

Figure 1. Geographic location of AERONET sites (red) in MODIS true color image of mainland China. The AERONET sites are divided into northern, southern, and western China as shown in the dashed boxes.

AERONET Lidar ratio and depolarization ratio to validate MISR nonspherical AOD. To raise the representativity of satellite results, spatial mean of MISR retrievals for comparison is selected only when more than five pixels are available.

3. Results and Analysis

3.1. General Performance of V23 MISR Aerosol Products Over East Asia

The high-resolution V23 MISR aerosol products provide a great chance to examine aerosol types in regional scales. To have a direct view on the performance of MISR retrievals in typical cases, we present the aerosol optical and microphysical parameters for a common clear day over eastern China on 17 May 2012 (Figure 2a). Compared with previous V22 MISR products with a resolution of 17.6 km (Kahn & Gaitley, 2015), V23 MISR AODs reveal detailed features such as the air pollution hot spot in urban region of Beijing at a much finer scale (Figure 2b). Although it seems clean in eastern China, the MISR AOD map shows notable aerosol plumes around cities and fires, especially over the bare land in northern China. In addition, MISR retrievals exhibits an overstrict cloud screening criterion to filter out changing aerosols near clouds (Varnai & Marshak, 2011), which in turn misses the dense smoke plumes and some clear places around clouds.

Figure 2c shows MISR aerosol mixtures classified into three broad types. The spherical nonabsorbing aerosols in the Mixture Group 1–30 are prevalent in eastern China, and their contribution to the total AOD is predominant in most areas (Figure 2d). It can be seen that MISR retrievals can identify absorbing particles around biomass burning plumes, with high absorption AODs around 0.3. However, there are only a few sporadic spherical absorbing AODs in eastern China (Figure 2e), indicating that MISR retrievals may be not sensitive enough to moderate-absorbing particles (Che et al., 2019; Tao, Wang, et al., 2017). Also, spatial distribution of MISR spherical absorbing AODs displays no apparent dependence on AOD and urban/industrial sources.

Particle size is an effective indicator of aerosol sources. Small-mode particles from anthropogenic sources and fire emissions have dominant contribution to the moderate to high AOD (>0.5) in eastern China (Figure 3a). Dust mixture is found in urban region of Beijing and central China (Figure 3d), which can be associated with the local wind-blown and long-range transport dust in spring. While nonspherical and dust component AOD shows obvious dust plumes in central China, these dust particles are mainly in small and medium modes mixed with local emissions. By contrast, high large-mode AOD (~0.3) values are

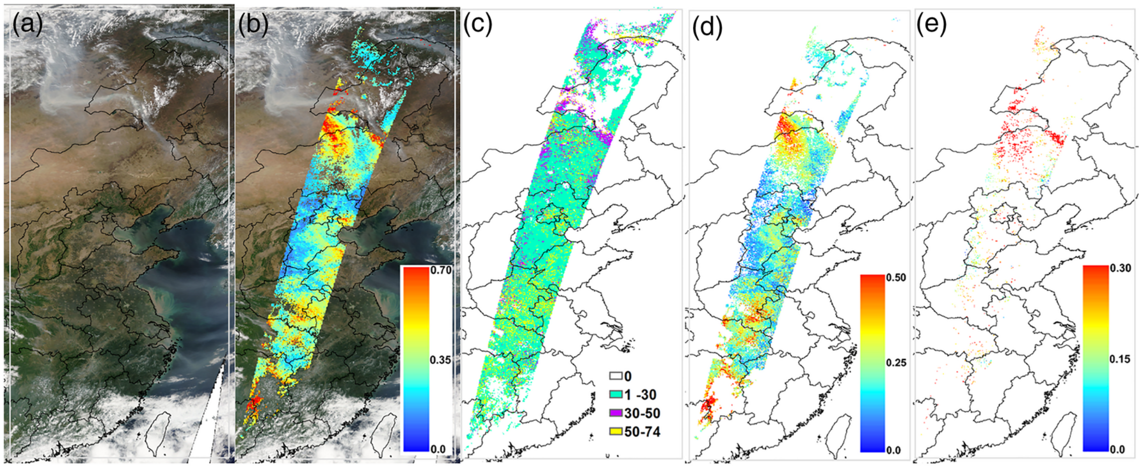

Figure 2. (a) Terra MODIS true color image, (b) MISR AOD, (c) MISR retrieved mixture group, (d) spherical nonabsorbing AOD, and (e) spherical absorbing AOD at 550 nm over eastern China on 17 May 2012.

concentrated in the eastern part of MISR image (Figure 3d) but are retrieved as spherical nonabsorbing particles rather than nonspherical dust, which needs to be verified by more observations.

To further examine the performance of MISR retrievals of dust particles, Figure 4 illustrates a typical case in the summer of 2006 over Taklimakan desert. Despite no visible aerosol plumes over the bright surface (Figure 4a), MISR AOD shows several regions with considerable aerosol loading (>0.5). The regional high AOD to the north of Taklimakan desert is dominated by small-mode particles, but coarse-mode AOD account for a large fraction in its eastern edge (Figure 4d), where dust sources can be located due to a limited transport potential of floating coarse particles. By contrast, large-mode dust has a higher fraction in the Taklimakan desert and exhibits prevalent nonspherical features. MISR retrievals identify the dust component in Taklimakan desert but take the aerosol plumes to the north as spherical nonabsorbing particles (Figure 4f). Generally, MISR aerosol type products show abundant information over deserts with a reasonable distribution.

Figure 5 shows a comparison of MISR and AERONET AOD as well as their Angstrom exponent (AE) at 860/550 and 675/440 nm, respectively, in the three typical regions. The V23 MISR AOD exhibits higher accuracy with ~80% of its retrievals falling within the expected error envelop of $\pm(0.05 + 20\%\mathrm{AOD}_{\mathrm{AERONET}})$ relative to the V22 (~75%) products (Kahn et al., 2010). Different from the scattered values in V22 retrievals, nearly all V23 MISR low to moderate AOD values (<0.6) in northern and southern China are within

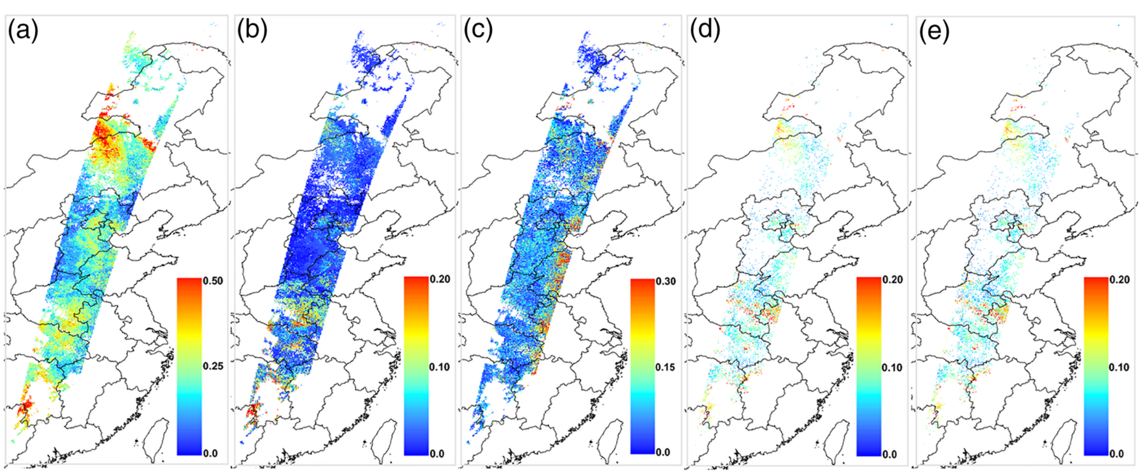

Figure 3. Same as Figure 2 but for AOD of (a) MISR small-mode, (b) medium-mode, (c) large-mode, (d) nonspherical, and (e) dust components at 550 nm.

10.1029/2019JD031909

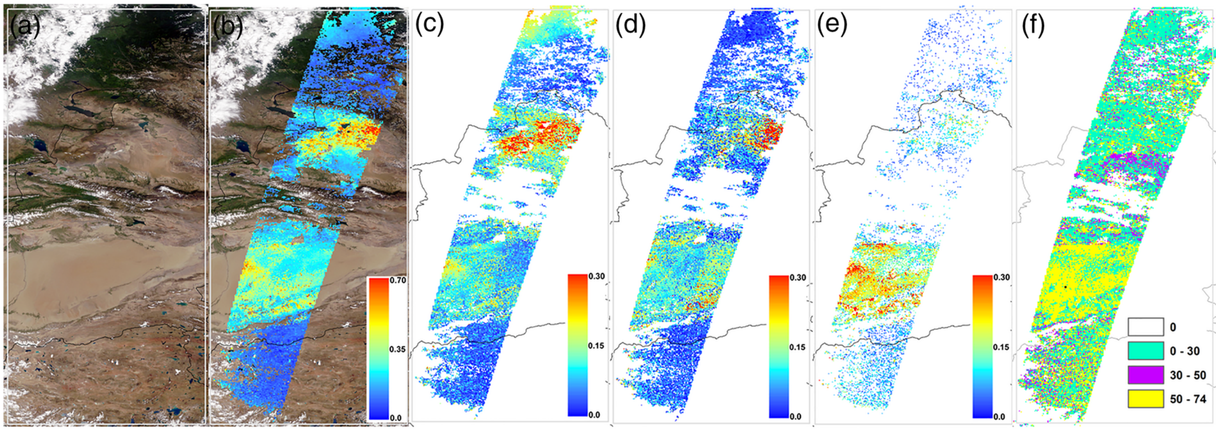

Figure 4. (a) Terra MODIS true color image, (b) MISR AOD, (c) small-mode AOD, (d) large-mode AOD, (e) nonspherical AOD, and (f) MISR retrieved mixture group over western China on 23 July 2006.

expected error range. The accuracy of V23 MISR AOD (78.5–83.8%) here is consistent with that found in the validation study (80.92%) of AERONET-DRAGON (Garay et al., 2017). Better consideration of spatial variation of aerosols at high resolution can be the main cause of this improvement.

However, a prominent underestimation still exists and the bias increases systematically with aerosol loading as in the V22 MISR products. As shown in Figure 2, few absorbing mixtures being selected in MISR retrievals can overestimate aerosol scattering contribution to TOA radiance, especially in high-AOD conditions. Accordingly, performance of MISR AOD is better in southern China than that in northern China, where weak-absorbing (SSA_{440}: 0.90–0.95) and moderate-absorbing (SSA_{440}: 0.85–0.90) aerosols are predominant, respectively (Tao, Wang, et al., 2017). In contrast, some MISR AOD retrievals are slightly overestimated over Dalanzadgad site with mixed surface types of bare land, desert, and vegetation. Meanwhile, MISR AODs in Baotou and SACOL exhibit similar accuracy as that in eastern China except an underestimation appearing for a lower AOD of ~0.4.

As the most widely used qualitative parameter regarding aerosol size, AE of MISR at 860/550 nm and AERONET at 675/440 nm are directly compared. Variations of AERONET AE reveal distinct particle types

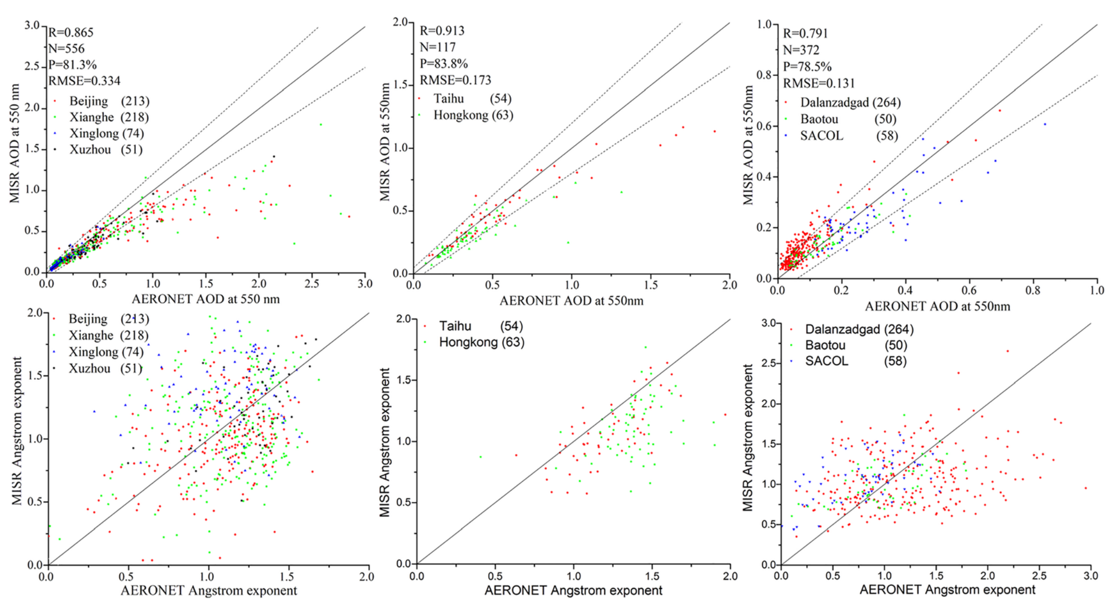

Figure 5. Scatter plots of MISR and AERONET AOD at 550 nm and their Angstrom exponent for 860/550 and 675/440 nm, respectively. The dashed and black lines are expected errors envelop (EE) of ±(0.05 + 20%) and 1-1 line. Correlation coefficient (R) and number (N) of matchups, percentage (P) within the EE, and root-mean-square error (RMSE) are also shown.

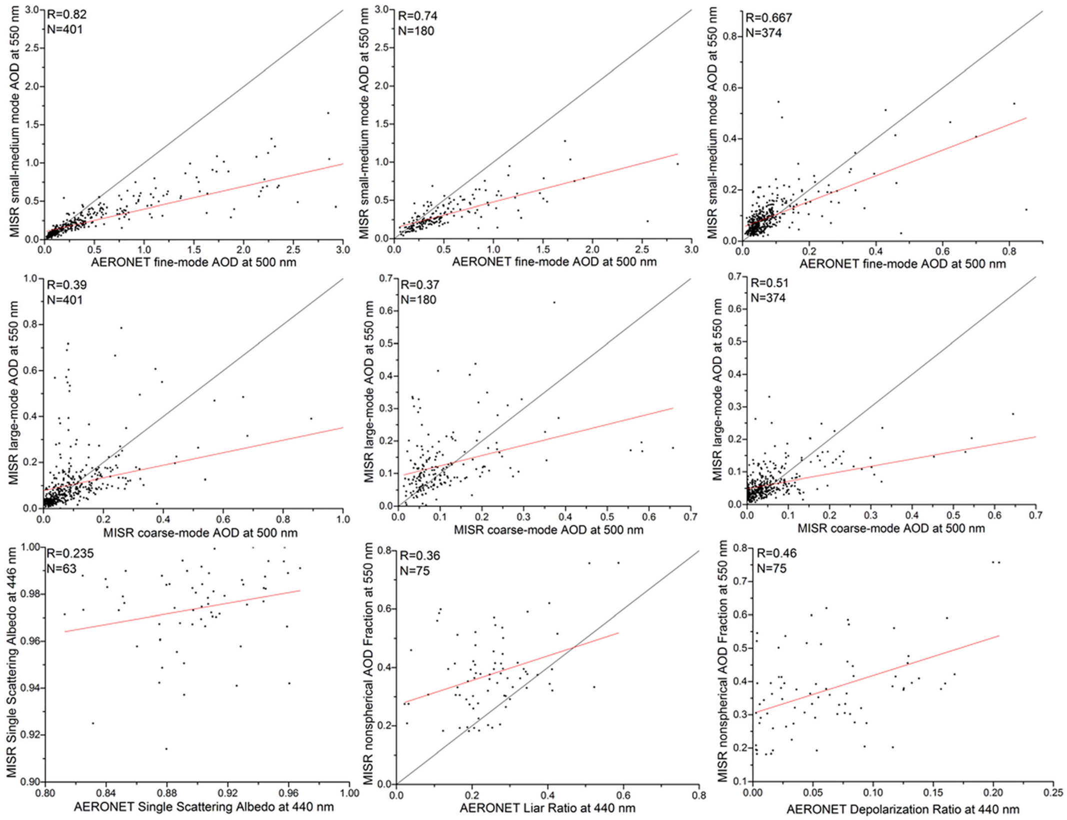

Figure 6. Scatter plots of MISR small-to-medium and large-mode AODs at 550 nm and AERONET fine- (top) and coarse-mode AODs (middle) at 500 nm, respectively, in northern, southern, and western China (left to right); all the MISR SSA at 446 nm and AERONET SSA at 440 nm, and fraction of MISR nonspherical AOD at 550 nm and AERONET Lidar ratio and depolarization ratio at 440 nm (bottom). The black and red lines denote 1-1 and linear fitting line.

in northern, southern, and western China. The mixture of fine anthropogenic aerosols and coarse natural dust is predominated in northern China with AE values ranging in 0.5–1.5 (Tao, Wang, et al., 2017). By contrast, AE is mostly higher than 1.0 in southern China, which is less influenced by dust transport. Although coarse dust prevails in western China (Tao, Chen, et al., 2017), most AE values within 0.5–1.5 indicate prevalent mixing of urban/industrial emissions and dust particles in western China. Similar as previous validations (Kahn et al., 2010), MISR retrievals tend to overestimate low AE (<1.0) values in western China and underestimate high AE (>1.0) vales in southern China. For northern China with hybrid aerosol types and large seasonal variations, both overestimation and underestimation exist in the MISR AE values.

To obtain a quantitative evaluation of MISR particle size, we compare the MISR small- and medium-mode AODs with AERONET fine-mode AOD, as well as the MISR large-mode AOD with the AERONET coarse mode (Figure 6). Consistent with ground validation of the total AOD, there is a high correlation between MISR and AERONET AOD at similar size modes in low to moderate values, indicating that MISR retrievals can reliably distinguish fine and coarse particles. Also, an underestimation appears in MISR small- and medium-mode AODs as aerosol loading increases, which can be caused by the underestimation of total AOD. Although most MISR large-mode AOD values are close to AERONET results, a notable overestimation and an underestimation exist below and above 0.1, separately. The dynamic separation point of fine and coarse modes in AERONET inversion can also impact the comparison.

Since reliable AERONET inversion of SSA requires a moderate to high aerosol loading ($AOD_{440} > 0.4$) and large solar zenith angle (>50°), there are much fewer matchups of MISR and AERONET SSA than those of AOD. A noticeable correlation is found between MISR and AERONET SSA (Figure 6), demonstrating that multiangle observation of MISR has a nonnegligible sensitivity to aerosol absorption. However, MISR SSA values are much higher (~0.05–0.10) than the AERONET results, which is accompanied by an underestimation of AOD. On the other hand, a linear correlation exists between the fraction of MISR nonspherical AOD

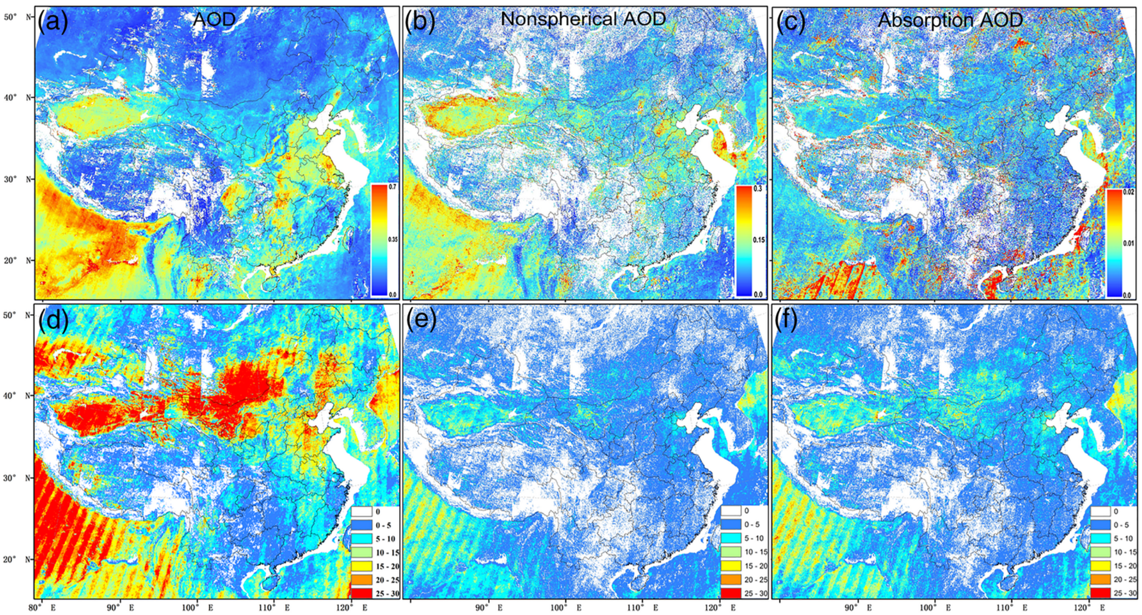

Figure 7. Annual mean of (a) MISR AOD, (b) nonspherical AOD, (c) absorption AOD at 550 nm, and their available retrieval frequency (d–f) in 2018.

and AERONET Lidar ratio as well as depolarization ratio, suggesting that MISR retrievals can reflect the contribution of nonspherical particles in the columnar AOD.

3.2. Characterization of Aerosol Type Over East Asia With MISR Retrievals

To characterize the spatial pattern of aerosol type over East Asia, annual means of MISR's total, nonspherical, and absorption AODs as well as their corresponding retrieval frequencies during 2018 are shown in Figure 7. MISR AOD distribution is consistent with that of MODIS products (Wei et al., 2019) and displays prominent hot spots in megacities such as Zhengzhou and Wuhan. The nonspherical AOD is highest in Taklimakan desert with several discrete high-value (~0.3) regions in northern China. MISR absorption AOD is generally very low (<0.01) except some high values (>0.02) in southern and northeastern China, possibly caused by biomass burning fires. For nonspherical and absorption AOD, their available retrievals are much sparser than MISR AOD, with no more than 5 days in most areas of eastern China. It is worth noting that nonspherical AOD only accounts for less than half of all MISR retrievals in Taklimakan desert, which can be caused by inappropriate dust models (Kahn et al., 2010). Moreover, there is a considerable decrease in the frequency of MISR AOD if only >0.15 cases are selected (supporting information Figure S1), in which the sensitivity of MISR retrievals to aerosol type is believed to improve largely (Kahn & Gaitley, 2015).

By comparison, MISR AODs of different size modes have a same temporal coverage as the total AOD (Figure S1). Figures 8a–8c shows the annual mean of MISR small-, medium-, and large-mode AODs during 2018, respectively. The distinct spatial patterns of small-mode and large-mode AODs show a marked contrast in aerosol types between eastern China and Taklimakan desert. The high values (>0.3) of small-mode AOD clearly reveal pollution hot spots in eastern China, while large-mode AOD can well reflect distribution of dust particles concentrated in the desert. Moreover, large-mode AOD exhibits an outstanding high value over the megacity, Zhengzhou. Ground $PM_{2.5}$ and PM_{10} in megacities of Beijing, Zhengzhou, and Wuhan around MISR passing time are compared to examine the cause (Figure 9). In accordance with MISR retrievals, it can be seen that both PM_{10}-dominant ($PM_{2.5}/PM_{10} < 0.6$) and high-PM_{10} (>150 μg/^{3}) days in Zhengzhou are evidently more frequent than these in Beijing and Wuhan. High values of medium-mode AOD (>0.15) are mostly distributed in central China, where humid environment can favor the hygroscopic growth of fine particles. The MISR aerosol size products with a reliable performance can effectively discriminate anthropogenic emissions from natural dust, which are dominated by small- and large-mode aerosols separately.

10.1029/2019JD031909

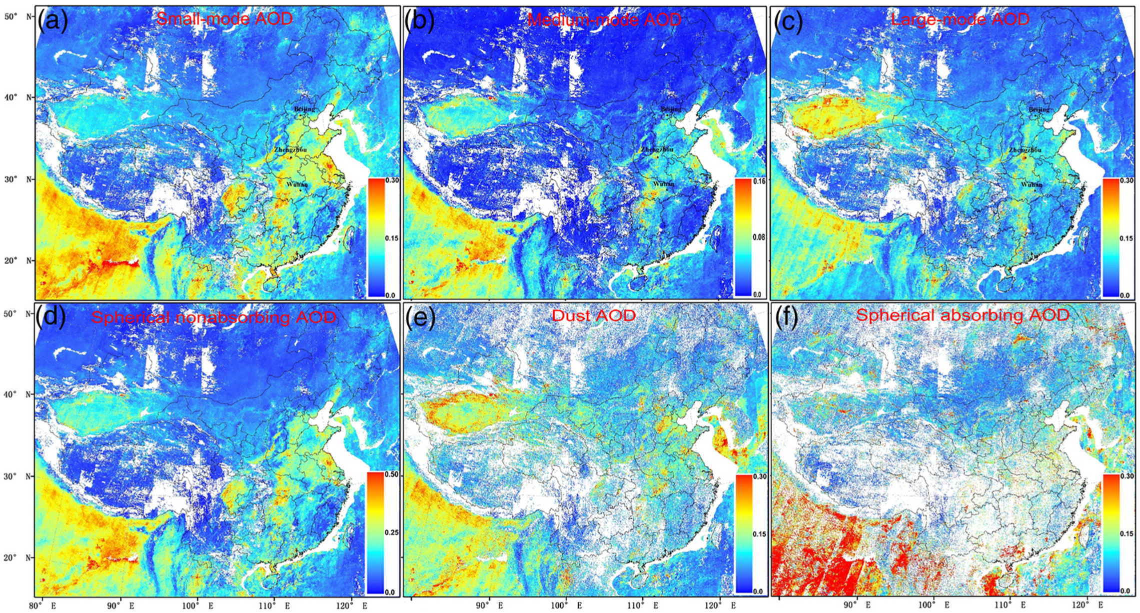

Figure 8. Annual mean of MISR (a) small-mode, (b) medium-mode, (c) large-mode, and (d) spherical nonabsorbing, (e) dust, and (f) spherical absorbing AODs at 550 nm in 2018.

The spherical nonabsorbing AOD has a very similar spatial distribution with the small-mode one except for higher magnitude (Figures 8a and 8d). Despite similar spatial pattern in Taklimakan desert, retrieval frequency of dust AOD is much lower than that of the large spherical nonabsorbing (2.8 μm) particles (Figure S2). The high values (>0.3) of annual dust AOD in eastern China can result from certain dust events with low representativity. MISR large-mode AOD is suggested as an indicator for dust particles (Kahn et al., 2010). On the other hand, annual mean of spherical absorbing AOD has a poor spatial coverage (Figure 8f), with no retrievals in the most part of central and southern China (Figure S3). Consistent with Figure 2e, spatial pattern of spherical absorbing AOD exhibits no clear connection with the total AOD or urban/industrial sources except for some hot spots (>0.3) near the biomass burning areas.

Considering the low frequency of MISR retrievals in a single year, seasonal average of MISR products during 2013–2018 is selected to further characterize the spatial variations of aerosol type (Figure 10). Seasonal MISR AOD exhibits a similar distribution as MODIS results (Tao et al., 2015), with distinct spatial and temporal changes. MISR fraction AOD at different size modes gives key information concerning aerosol sources. The small-mode AOD reveals the seasonal patterns of anthropogenic particles in eastern China driven by dynamic meteorological conditions. High large-mode AOD (>0.5) shows that the dust events in western China are active in spring and summer, but dust transport mainly occurs in spring with prevailing northwestern winds. There is a clear dust transport belt between Taklimakan desert and northern China during spring with large-mode AOD > 0.3, and coarse particles account for more than half of the MISR AOD in northern China. MISR AOD hot spots (>0.7) over northern China in summer and southern China in spring are dominated by small-mode particles from urban/industrial smog and fire smoke, respectively. Also, it is found that large- and small-mode aerosols play a major contribution to AOD hot spots over central China during winter and fall separately.

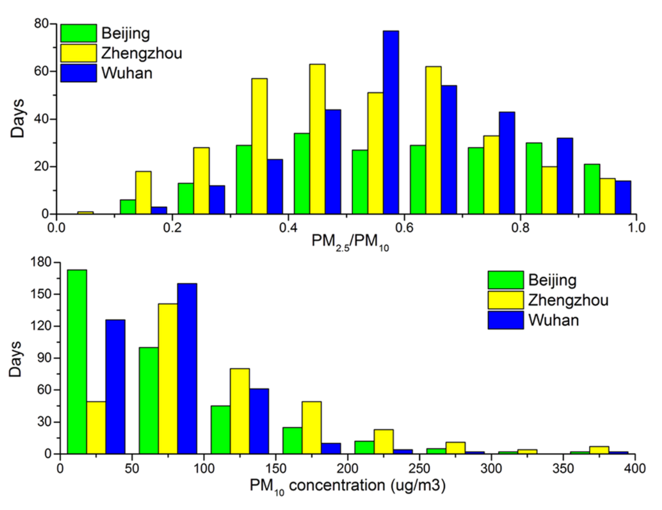

Figure 9. Annual frequency of $PM_{2.5}/PM_{10}$ ratio (top) and PM_{10} concentration (bottom) in Beijing, Zhengzhou, and Wuhan within 1 hr of MISR passing time during 2018.

The MISR component AOD provides more information regarding major aerosol hot spots (Figure 11). MISR dust and spherical absorbing AOD clearly show seasonal variation of dust activities and fire smoke. Besides spring, dust AOD is relatively high (>0.2) over central China in winter

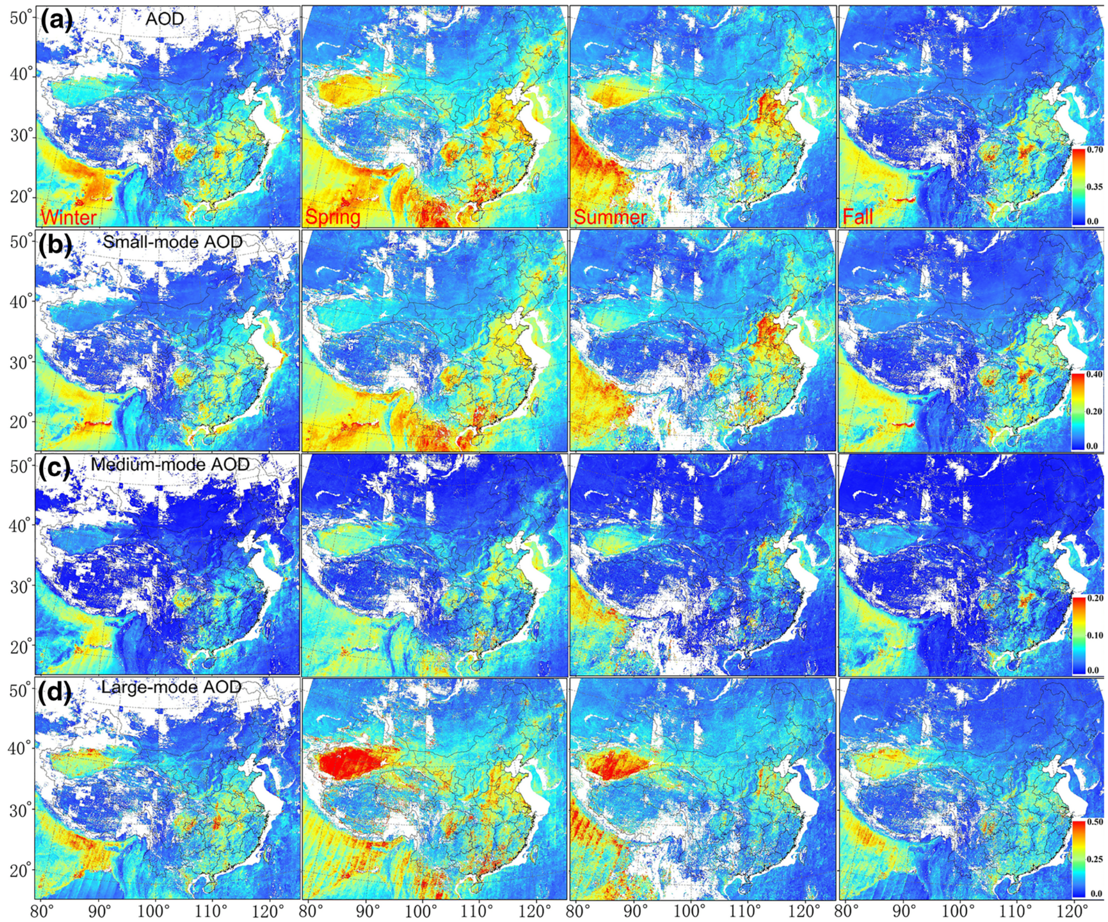

Figure 10. Seasonal mean of MISR (a) AOD, (b) small-mode, (c) medium-mode, and (d) large-mode AODs at 550 nm during 2013–2018.

and in northern China during summer. High spherical absorbing AOD (>0.3) reflects fire smoke plumes over northeastern China and southern China with notable seasonal variations. By contrast, spherical nonabsorbing aerosols are mainly concentrated in the urban/industrial areas. Despite better spatial coverage than annual mean in a single year, seasonal spherical absorbing AOD values during 2013–2018 remain discrete without notable self-consistency. MISR component AODs have higher uncertainties than AODs for individual size bins even for the three broad categories, due mostly to the inappropriate aerosol models used (Kahn et al., 2010; Kahn & Gaitley, 2015).

Figure 12 illustrates the daily variation of aerosol mixtures selected in MISR retrievals over Beijing, Hong Kong, and one dust hot spot over deserts. Consistent with AERONET observations (Tao, Wang, et al., 2017), spherical nonabsorbing aerosols and nonspherical dust are prevalent in northern China. The spherical absorbing retrievals are much fewer, and barely exist in summer, when weak-absorbing particles prevail with high SSA values (~0.90–0.95). By contrast, MISR retrievals in Hong Kong is dominated by spherical nonabsorbing mixtures and accompanied with some absorbing ones in winter. Large-mode aerosols are predominant in the deserts and generally fall into two classes including spherical nonabsorbing and dust mixtures. While MISR dust component tends to be concentrated in the edge area of Taklimakan desert, large spherical particles are mainly distributed in the center of the desert (Figure S3). The limited fraction of nonspherical retrievals can partly explain the large underestimation of MISR dust AOD over East Asia compared with model simulations (Lee et al., 2016).

3.3. Application Potential and Uncertainties of MISR Products Over East Asia

Compared with the current operational satellite aerosol products usually with one quantitative parameter of AOD, the high-resolution V23 MISR aerosol type retrievals provide additional optical and microphysical

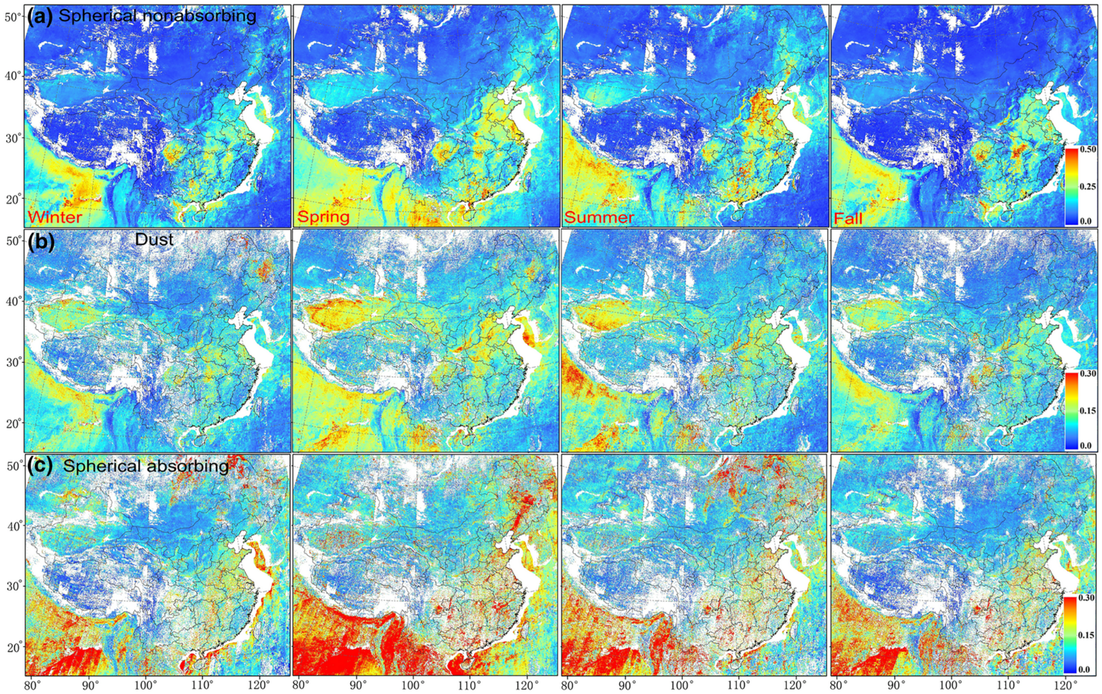

Figure 11. Seasonal mean of MISR (a) spherical nonabsorbing, (b) dust, and (c) spherical absorbing component AODs at 550 nm during 2013–2018.

information associated with particle sources, composition, and evolution in the regional scales. Despite remarkable improvement in MISR AOD retrievals, V23 MISR aerosol type products are subject to similar uncertainties as found in V22 retrievals due to the same algorithm principle being used (Kahn et al., 2010; Kahn & Gaitley, 2015). In particular, ground validation and spatial analysis over East Asia enable a more detailed insight into the application potential and error sources of MISR retrievals.

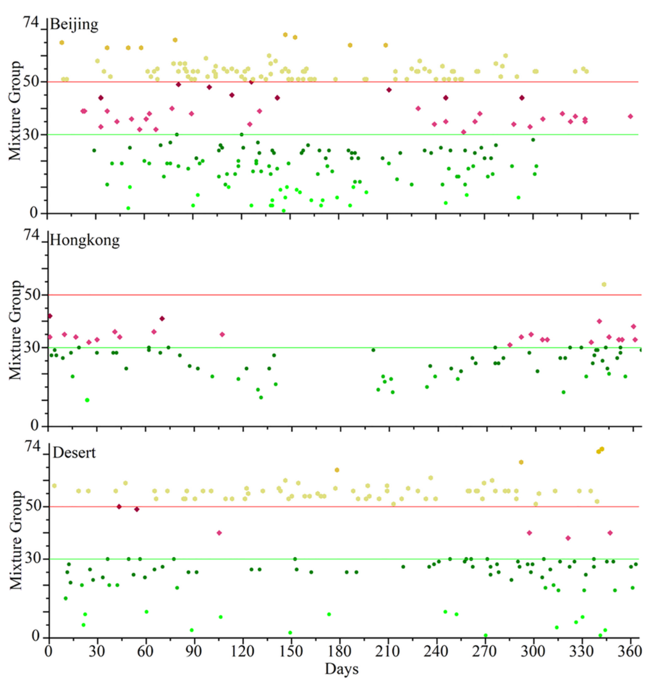

Figure 12. Daily variation of selected aerosol mixtures in MISR retrievals in Beijing, Hong Kong, and location (85°E, 38°N) of dust hot spot in Taklimakan desert. The green, red, and brown dots denote spherical nonabsorbing, spherical absorbing, and nonspherical aerosol mixtures, respectively.

Surface-atmosphere separation problem is considered as the primary cause of MISR AOD underestimation when SSA is near or equal to 1.0 (Kahn et al., 2010), which assigns some atmospheric signals to the surface. The evident improvement in accuracy of V23 MISR AOD demonstrates that the assignment of subscale AOD variability within V22's 17.6 km retrieval region to surface has a considerable influence on AOD retrievals (Limbacher & Kahn, 2014). Moreover, MISR AOD exhibits different performances in typical regions of East Asia with distinct aerosol properties (Figure 5). The aerosols in northern China are characterized by a mixture of moderate-absorbing anthropogenic particles and prevalent dust (Tao, Wang, et al., 2017), which is not included in the current MISR 74 mixtures (Kahn et al., 2010). Thus, the most commonly used nonabsorbing mixtures in MISR retrievals can also have an important contribution to the AOD errors in northern China. By comparison, the underestimation of MISR AOD is much smaller in southern China, where spherical weak-absorbing aerosols prevail.

Compared with the annual MODIS AOD at 10 km in northern China during 2018, V23 MISR retrievals show notable pollution hot spots over the urban and industrial regions at a finer scale (Figure 13). MISR AOD can even reflect the location of downtown area characterized by ring roads in the megacity of Beijing. By contrast, MODIS AOD is much higher (~0.2–0.3) in the North China Plain but is obviously lower in central China. The considerable underestimation of MISR AOD in high values

10.1029/2019JD031909

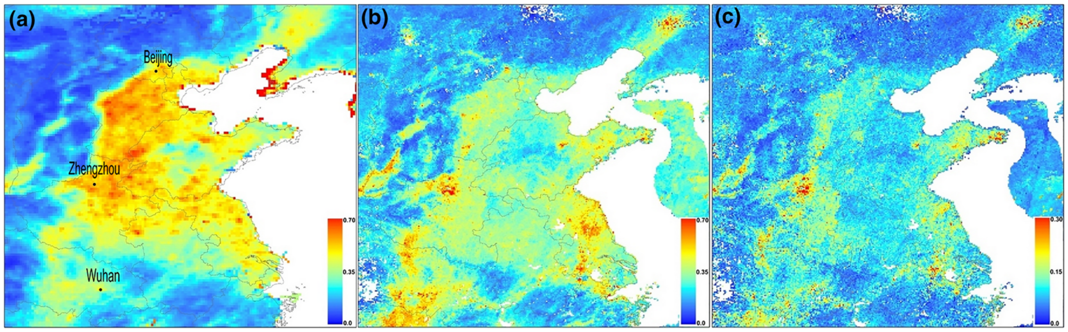

Figure 13. Annual mean value of (a) Collection 6.1 MODIS Deep Blue AOD, (b) MISR AOD, and (c) large-mode AOD at 550 nm during 2018.

(>0.6) can be part of the reason. Also, the low retrieval frequency of MISR AOD can miss some high-AOD events or take few of them as the main signal (Tao et al., 2015). Despite these limitations, MISR retrievals have greatly renewed the cognition of aerosol type information in addition to the conventional satellite AOD. For instance, the MISR large-mode AOD in northern China exhibits marked hot spots in several urban/industrial areas, where emissions related to coarse particles such as construction can be active.

To explore the temporal representativity of MISR aerosol products, collocated MISR and AERONET AOD and SSA over Beijing are compared on a monthly scale during 2001–2018 (Figure 14). Despite very different sampling frequency, long-term variations of MISR AOD and SSA generally exhibit consistent trends with those of AERONET. With stringent emission reduction measures, there has been a significant decrease in aerosol loading and absorbing components such as black carbon in Beijing (Lyapustin et al., 2011; Zhang et al., 2019). It should be stated that spatial average of the very sparse and discrete SSA values <1.0 can still capture the temporal changes in aerosol absorption as AERONET. Since the selection of absorbing mixture in MISR retrievals seems have no obvious connection with AOD or location of emission sources in eastern China (Figures 2e and 8f), whether the sparse absorbing retrievals are caused by inappropriate aerosol models or algorithm artifacts should be confirmed in the future refinement. Consistent with aforementioned validation, large difference exists in the magnitude of AOD and SSA between MISR and AERONET results, especially for their high values.

Compared with the operational MODIS AOD that has considerable bias over the deserts of East Asia (Tao et al., 2015; Tao, Chen, et al., 2017), MISR retrievals with robust performance over bright surface show prominent advantage in characterizing the spatial pattern of airborne dust over Taklimakan desert (Figure 15).

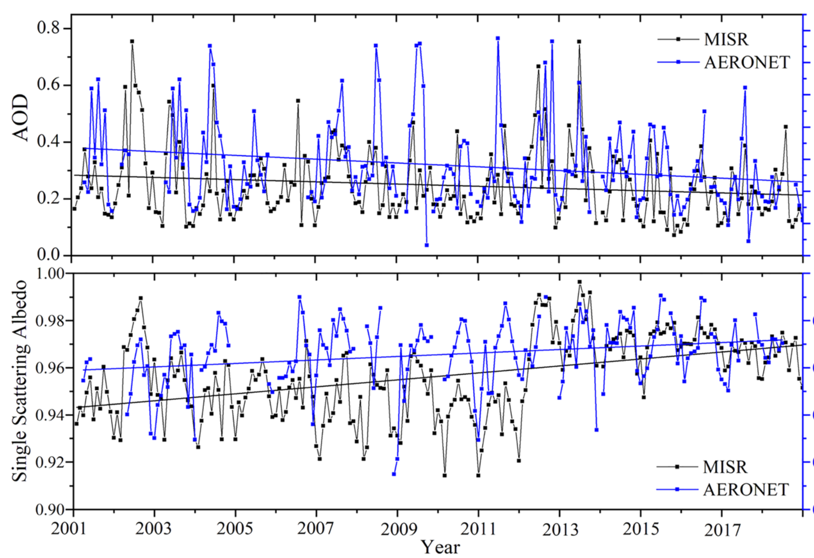

Figure 14. Time series variations of monthly mean of MISR and AERONET AOD at 550 nm (top), and MISR and AERONET single scattering albedo at 446 and 440 nm during 2001–2018 (bottom).

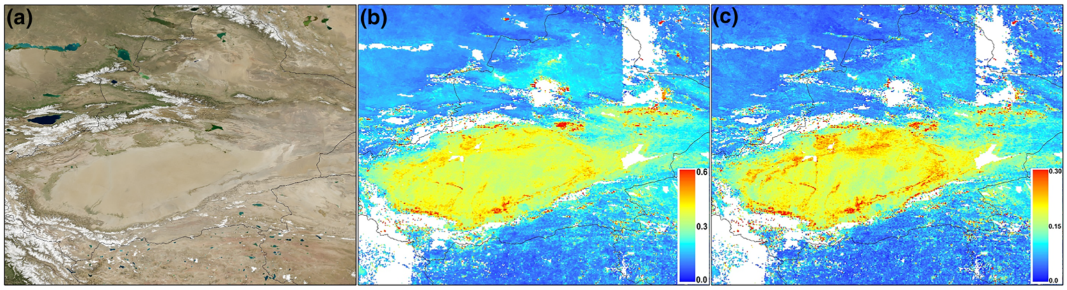

Figure 15. (a) MODIS true color image, mean value of (b) MISR AOD, and (c) large-mode AOD at 550 nm over Taklimakan desert during 2014–2018.

The annual mean of MISR large-mode AOD shows clear hot spots of dust activities, which is consistent with the spatial distribution of aerosol loading. It can be seen that the dust events are mainly concentrated along the oasis and rivers rather than the center of Taklimakan desert. The satellite information concerning dust sources and activities can constrain dust emission estimates and verify uplifting mechanisms of model simulations concerning their climate effects.

In general, the high-resolution V23 MISR products show a great application potential in aerosol researches with regard to air quality and climate effects in the regional scales. The long-term multiangle MISR observation can largely bridge the data gap between model simulations and conventional satellite AOD products with additional aerosol type information. However, the lack of aerosol component models with appropriate particle size and also their mixtures has obstructed the reliability of MISR aerosol type products over East Asia. With extensive modification tests, the MISR research aerosol retrieval algorithm over water has shown a promising feasibility in refining MISR retrievals with expanded aerosol mixtures and other well-considered factors (Limbacher & Kahn, 2014, 2019). According to the spatial pattern of aerosol properties, adopting specific aerosol mixtures in divided regions such as East Asia could improve MISR retrievals without overmuch increase in computing cost. Based on the evident advantage of MISR multiangle retrievals, the MAIA instrument with much wider spectrum range and additional polarimetry will provide significantly enhanced detection of aerosol type information.

4. Conclusions

The quantitative aerosol products over land from the common single-view and multiband satellite instruments usually only include AOD, which has been the most widely used aerosol parameter due to their near-daily global coverage and high spatial resolution. However, the lack of aerosol type information has hindered further applications of these operational satellite products such as constraining model simulations, inferring specific emissions sources, and quantifying aerosol climate effects. With the advantage of multiangle measurements, MISR products include abundant particle optical and microphysical parameters regarding aerosol type. In particular, recent V23 MISR aerosol products have raised their spatial resolution from original 17.6 to 4.4 km. In this study, we provide a comprehensive insight into the capability and reliability of V23 MISR retrievals in characterizing aerosol types over East Asia.

Despite the same algorithm principle as V22, ground validation shows an evident improvement in the accuracy of V23 MISR AOD, with ~80% of its retrieval errors within $\pm(0.05 + 20\%\mathrm{AOD_{AERONET}})$ relative to the V22 (~75%) products. However, a considerable underestimation remains prevalent in high-AOD (>0.6) conditions. The surface-atmosphere separation problem could be the main cause of MISR AOD underestimation when SSA is close or equal to 1.0. The V23 MISR retrievals at a higher resolution obviously reduced the influence of AOD variability within the V22's 17.6 km retrieval region, which can be assigned to the surface. Meanwhile, MISR retrievals mostly take the prevalent moderate-absorbing aerosols as nonabsorbing mixtures, which can also contribute to this underestimation.

MISR AOD at three size modes tends to be a reliable indicator in discriminating different aerosol types such as anthropogenic emissions from natural dust. Also, MISR SSA and nonspherical AOD values exhibit consistent variations with AERONET inversions. However, V23 MISR component AOD retrievals exhibit marked difference with the general expectation over East Asia. The lack of appropriate aerosol component models and their mixtures as found in the V22 products has largely hampered accurate discrimination of aerosol types. Nonspherical mixtures only account for less than half of the MISR retrievals over Taklimakan desert. The most prominent problem is the very sparse MISR absorbing retrievals except over intensive fire smoke. Despite these limitations, MISR retrievals generally capture the distinct spatial and temporal features of aerosol type in typical regions of East Asia. Motivated by the promising feasibility of MISR research aerosol retrieval algorithm, further refinements of the MISR retrievals with more realistic assumptions have a great application potential in quantifying the role of aerosols in regional air quality and climate.

Data Availability Statement

The original MISR aerosol products can be downloaded from the website (https://misr.jpl.nasa.gov/getData/accessData/) by registering a user account for free. The AERONET data can be directly downloaded from the website freely (https://aeronet.gsfc.nasa.gov/new_web/index.html) without any registering information.

Acknowledgments

This study was supported by National Science Foundation of China (Grants 41830109, 41871262, and 41601472). J. Wang's participation is made possible through the in-kind support from the University of Iowa. We thank the MISR aerosol team (https://misr.jpl.nasa.gov) for the data used in our work. We acknowledge AERONET site PIs (B. N. Holben, H. Chen, L. Wu, R. Ma, J. E. Nichol, P. Wang, X. Xia, and Z. Li) for providing the aerosol data available.

References

Boucher, O., Randall, D., Artaxo, P., Bretherton, C., Feingold, G., Forster, P., et al. (2013). Clouds and aerosols. In Climate change 2013: The physical science basis. Contribution of Working Group I to the Fifth. In *Assessment Report of the Intergovernmental Panel on Climate Change* (pp. 571–657). Cambridge, UK: Cambridge University Press.

Che, H., Xia, X., Zhao, H., Dubovik, O., Holben, B. N., Goloub, P., et al. (2019). Spatial distribution of aerosol microphysical and optical properties and direct radiative effect from the China Aerosol Remote Sensing Network. *Atmospheric Chemistry and Physics*, *19*(18), 11,843–11,864.

Chen, C., Dubovik, O., Henze, D. K., Lapyonak, T., Chin, M., Ducos, F., et al. (2018). Retrieval of desert dust and carbonaceous aerosol emissions over Africa from POLDER/PARASOL products generated by the GRASP algorithm. *Atmospheric Chemistry and Physics*, *18*(16), 12,551–12,580. https://doi.org/10.5194/acp-18-12551-2018

Chen, T., Guo, J., Li, Z., Zhao, C., Liu, H., Cribb, M., et al. (2016). A CloudSat perspective on the cloud climatology and its association with aerosol perturbations in the vertical over eastern China. *Journal of the Atmospheric Sciences*, *73*(9), 3599–3616. https://doi.org/10.1175/JAS-D-15-0309.1

Christian, K., Wang, J., Ge, C., Peterson, D., Hyer, E., Yorks, J., & McGill, M. (2019). Radiative forcing and stratospheric warming of pyrocumulonimbus smoke aerosols: First modeling results with multisensor (EPIC, CALIPSO, and CATS) views from space. *Geophysical Research Letters*, *46*, 10,061–10,071. https://doi.org/10.1029/2019GL082360

Christopher, S. A., & Wang, J. (2004). Intercomparison between multi-angle imaging spectroradiometer (MISR) and sunphotometer aerosol optical thickness in dust source regions over China: Implications for satellite aerosol retrievals and radiative forcing calculations. *Tellus B*, *56*(5), 451–456.

Diner, D. J., Boland, S. W., Brauer, M., Bruegge, C., Burke, K. A., Chipman, R., et al. (2018). Advances in multiangle satellite remote sensing of speciated airborne particulate matter and association with adverse health effects: From MISR to MAIA. *Journal of Applied Remote Sensing*, *12*(4), 042603.

Diner, D. J., Braswell, B. H., Davies, R., Gobron, N., Hu, J., Jin, Y., et al. (2005). The value of multiangle measurements for retrieving structurally and radiatively consistent properties of clouds, aerosols, and surfaces. *Remote Sensing of Environment*, *97*(4), 495–518. https://doi.org/10.1016/j.rse.2005.06.006

Ding, S., Wang, J., & Xu, X. (2016). Polarimetric remote sensing in oxygen A and B bands: Sensitivity study and information content analysis for vertical profile of aerosols. *Atmospheric Measurement Techniques*, *9*(5), 2077–2092. https://doi.org/10.5194/amt-9-2077-2016

Dubovik, O., Holben, B., Eck, T. F., Smirnov, A., Kaufman, Y. J., King, M. D., et al. (2002). Variability of absorption and optical properties of key aerosol types observed in worldwide locations. *Journal of the Atmospheric Sciences*, *59*(3), 590–608. https://doi.org/10.1175/1520-0469(2002)059<0590:VOAAOP>2.0.CO;2

Dubovik, O., Holben, B. N., Lapyonok, T., Sinyuk, A., Mishchenko, M. I., Yang, P., & Slutsker, I. (2002). Non-spherical aerosol retrieval method employing light scattering by spheroids. *Geophysical Research Letters*, *29*(10), 1451. https://doi.org/10.1029/2001GL014506

Dubovik, O., & King, M. D. (2000). A flexible inversion algorithm for retrieval of aerosol optical properties from Sun and sky radiance measurements. *Journal of Geophysical Research*, *105*(D16), 20,673–20,696. https://doi.org/10.1029/2000JD900282

Dubovik, O., Li, Z., Mishchenko, M. I., Tanré, D., Karol, Y., Bojkov, B., et al. (2019). Polarimetric remote sensing of atmospheric aerosols: Instruments, methodologies, results, and perspectives. *Journal of Quantitative Spectroscopy and Radiative Transfer*, *224*, 474–511. https://doi.org/10.1016/j.jqsrt.2018.11.024

Eck, T. F., Holben, B. N., Reid, J. S., Dubovik, O., Smirnov, A., O'Neill, N. T., et al. (1999). Wavelength dependence of the optical depth of biomass burning, urban, and desert dust aerosols. *Journal of Geophysical Research*, *104*(D24), 31,333–31,349. https://doi.org/10.1029/1999JD900923

Fan, J., Leung, L. R., Li, Z., Morrison, H., Chen, H., Zhou, Y., et al. (2012). Aerosol impacts on clouds and precipitation in eastern China: Results from bin and bulk microphysics. *Journal of Geophysical Research*, *117*, D00K36. https://doi.org/10.1029/2011JD016537

Garay, M. J., Kalashnikova, O. V., & Bull, M. A. (2017). Development and assessment of a higher-spatial-resolution (4.4 km) MISR aerosol optical depth product using AERONET-DRAGON data. *Atmospheric Chemistry and Physics*, *17*(8), 5095–5106. https://doi.org/10.5194/acp-17-5095-2017

Garay, M. J., Witek, M. L., Kahn, R. A., Seidel, F. C., Limbacher, J. A., Bull, M. A., et al. (2020). Introducing the 4.4 km spatial resolution Multi-Angle Imaging SpectroRadiometer (MISR) aerosol product. *Atmospheric Measurement Techniques*, *13*(2), 593–628. https://doi.org/10.5194/amt-13-593-2020

Ge, C., Wang, J., Carn, S., Yang, K., Ginoux, P., & Krotkov, N. (2016). Satellite-based global volcanic SO2 emissions and sulfate directradiative forcing during 2005–2012. *Journal of Geophysical Research: Atmospheres*, *121*, 3446–3464. https://doi.org/10.1002/2015JD023134

Giles, D. M., Sinyuk, A., Sorokin, M. G., Schafer, J. S., Smirnov, A., Slutsker, I., et al. (2019). Advancements in the aerosol Robotic Network (AERONET) Version 3 database—Automated near-real-time quality control algorithm with improved cloud screening for Sun photometer aerosol optical depth (AOD) measurements. *Atmospheric Measurement Techniques*, *12*(1), 169–209. https://doi.org/10.5194/amt-12-169-2019

Guo, J., Deng, M., Lee, S., Wang, F., Li, Z., Zhai, P., et al. (2016). Delaying precipitation and lightning by air pollution over the Pearl River Delta. Part I: Observational analyses. *Journal of Geophysical Research: Atmospheres*, *121*, 6472–6488. https://doi.org/10.1002/2015JD023257

Holben, B. N., Eck, T. F., Slutsker, I., Tanré, D., Buis, J. P., Setzer, A., et al. (1998). AERONET—A federated instrument network and data archive for aerosol characterization. *Remote Sensing of Environment*, *66*(1), 1–16. https://doi.org/10.1016/S0034-4257(98)00031-5

Ichoku, C., Chu, D. A., Mattoo, S., Kaufman, Y. J., Remer, L. A., Tanré, D., et al. (2002). A spatio-temporal approach for global validation and analysis of MODIS aerosol products. *Geophysical Research Letters*, *29*(12), 8006. https://doi.org/10.1029/2001GL013206

Kahn, R., Banerjee, P., & McDonald, D. (2001). Sensitivity of multiangle imaging to natural mixtures of aerosols over ocean. *Journal of Geophysical Research*, *106*(D16), 18,219–18,238. https://doi.org/10.1029/2000JD900497

Kahn, R., Banerjee, P., McDonald, D., & Diner, D. J. (1998). Sensitivity of multiangle imaging to aerosol optical depth and to pure-particle size distribution and composition over ocean. *Journal of Geophysical Research*, *103*(D24), 32,195–32,213. https://doi.org/10.1029/98JD01752

Kahn, R. A., & Gaitley, B. J. (2015). An analysis of global aerosol type as retrieved by MISR. *Journal of Geophysical Research: Atmospheres*, *120*, 4248–4281. https://doi.org/10.1002/2015JD023322

Kahn, R. A., Gaitley, B. J., Garay, M. J., Diner, D. J., Eck, T. F., Smirnov, A., & Holben, B. N. (2010). Multiangle Imaging SpectroRadiometer global aerosol product assessment by comparison with the Aerosol Robotic Network. *Journal of Geophysical Research*, *115*, D23209. https://doi.org/10.1029/2010JD014601

Kaufman, Y. J., Tanre, D., & Boucher, O. (2002). A satellite view of aerosols in the climate system. *Nature*, *419*(6903), 215–223. https://doi.org/10.1038/nature01091

King, M. D., Kaufman, Y. J., Tanré, D., & Nakajima, T. (1999). Remote sensing of tropospheric aerosols from space: Past, present, and future. *Bulletin of the American Meteorological Society*, *80*(11), 2229–2259. https://doi.org/10.1175/1520-0477(1999)080<2229:RSOTAF>2.0.CO;2

Koren, I., Kaufman, Y. J., Remer, L. A., & Martins, J. V. (2004). Measurement of the effect of Amazon smoke on inhibition of cloud formation. *Science*, *303*(5662), 1342–1345. https://doi.org/10.1126/science.1089424

Lee, H., Kalashnikova, O. V., Suzuki, K., Braverman, A., Garay, M. J., & Kahn, R. A. (2016). Climatology of the aerosol optical depth by components from the Multi-angle Imaging SpectroRadiometer (MISR) and chemistry transport models. *Atmospheric Chemistry and Physics*, *16*(10), 6627–6640. https://doi.org/10.5194/acp-16-6627-2016

Li, S., Garay, M. J., Chen, L., Rees, E., & Liu, Y. (2013). Comparison of GEOS-Chem aerosol optical depth with AERONET and MISR data over the contiguous United States. *Journal of Geophysical Research: Atmospheres*, *118*, 11,228–11,241. https://doi.org/10.1002/jgrd.50867

Li, Z., Guo, J., Ding, A., Liao, H., Liu, J., Sun, Y., et al. (2017). Aerosol and boundary-layer interactions and impact on air quality. *National Science Review*, *4*(6), 810–833. https://doi.org/10.1093/nsr/nwx117

Li, Z., Wang, Y., Guo, J., Zhao, C., Cribb, M. C., Dong, X., et al. (2019). East Asian Study of Tropospheric Aerosols and their Impact on Regional Clouds, Precipitation, and Climate (EAST-AIRCPC). *Journal of Geophysical Research: Atmospheres*, *124*, 13,026–13,054. https://doi.org/10.1029/2019JD030758

Limbacher, J., & Kahn, R. A. (2014). MISR research-aerosol-algorithm refinements for dark water retrievals. *Atmospheric Measurement Techniques*, *7*(11), 3989–4007. https://doi.org/10.5194/amt-7-3989-2014

Limbacher, J. A., & Kahn, R. A. (2019). Updated MISR over-water research aerosol retrieval algorithm—Part 2: A multi-angle aerosol retrieval algorithm for shallow, turbid, oligotrophic, and eutrophic waters. *Atmospheric Measurement Techniques*, *12*(1), 675–689. https://doi.org/10.5194/amt-12-675-2019

Liu, J., Xia, X., Li, Z., Wang, P., Min, M., Hao, W., et al. (2010). Validation of multi-angle imaging spectroradiometer aerosol products in China. *Tellus B*, *62*(2), 117–124. https://doi.org/10.1111/j.1600-0889.2009.00450.x

Liu, Y., Koutrakis, P., & Kahn, R. (2007). Estimating fine particulate matter component concentrations and size distributions using satellite-retrieved fractional aerosol optical depth: Part 1—Method development. *Journal of the Air & Waste Management Association*, *57*(11), 1351–1359. https://doi.org/10.3155/1047-3289.57.11.1351

Liu, Z., Ming, Y., Zhao, C., Lau, N. C., Guo, J., Bollasina, M., & Yim, S. H. L. (2020). Contribution of local and remote anthropogenic aerosols to a record-breaking torrential rainfall event in Guangdong Province, China. *Atmospheric Chemistry and Physics*, *20*(1), 223–241. https://doi.org/10.5194/acp-20-223-2020

Lyapustin, A., Smirnov, A., Holben, B., Chin, M., Streets, D. G., Lu, Z., et al. (2011). Reduction of aerosol absorption in Beijing since 2007 from MODIS and AERONET. *Geophysical Research Letters*, *38*, L10803. https://doi.org/10.1029/2011GL047306

Martonchik, J. V., Kahn, R. A., & Diner, D. J. (2009). Retrieval of aerosol properties over land using MISR observations. In A. Kokhanovsky (Ed.), *Satellite aerosol remote sensing over land* (pp. 267–293). Berlin: Springer.

Meng, X., Garay, M. J., Diner, D. J., Kalashnikova, O. V., Xu, J., & Liu, Y. (2018). Estimating PM2.5 speciation concentrations using prototype 4.4 km-resolution MISR aerosol properties over Southern California. *Atmospheric Environment*, *181*, 70–81. https://doi.org/10.1016/j.atmosenv.2018.03.019

Pope, I. C., Burnett, R. T., Thun, M. J., et al. (2002). Lung cancer, cardiopulmonary mortality, and long-term exposure to fine particulate air pollution. *Journal of the American Medical Association*, *287*(9), 1132–1141. https://doi.org/10.1001/jama.287.9.1132

Tao, M., Chen, L., Wang, Z., Tao, J., Che, H., Wang, X., & Wang, Y. (2015). Comparison and evaluation of the MODIS Collection 6 aerosol data in China. *Journal of Geophysical Research: Atmospheres*, *120*, 6992–7005. https://doi.org/10.1002/2015JD023360

Tao, M., Chen, L., Wang, Z., Wang, J., Che, H., Xu, X., et al. (2017). Evaluation of MODIS Deep Blue Aerosol Algorithm in desert region of East Asia: Ground validation and intercomparison. *Journal of Geophysical Research: Atmospheres*, *122*, 10,357–10,368. https://doi.org/10.1002/2017JD026976

Tao, M., Wang, Z., Tao, J., Chen, L., Wang, J., Hou, C., et al. (2017). How do aerosol properties affect the temporal variation of MODIS AOD bias in eastern China? *Remote Sensing*, *9*(8), 800. https://doi.org/10.3390/rs9080800

Varnai, T., & Marshak, A. (2011). Global CALIPSO observations of aerosol changes near clouds. *IEEE Geoscience and Remote Sensing Letters*, *8*(1), 19–23. https://doi.org/10.1109/LGRS.2010.2049982

Wang, F., Guo, J., Zhang, J., Huang, J., Min, M., Chen, T., et al. (2015). Multi-sensor quantification of aerosol-induced variability in warm clouds over eastern China. *Atmospheric Environment*, *113*, 1–9. https://doi.org/10.1016/j.atmosenv.2015.04.063

Wang, J., Xu, X., Henze, K., Zeng, J., Ji, Q., Tsay, S.-C., & Huang, J. (2012). Top-down estimate of dust emissions through integration of MODIS and MISR aerosol retrievals with the GEOS-Chem adjoint model. *Geophysical Research Letters*, *39*, L08802. https://doi.org/10.1029/2012GL051136

Wang, Y., Khalizov, A., Levy, M., & Zhang, R. (2013). New directions: Light absorbing aerosols and their atmospheric impacts. *Atmospheric Environment*, *81*, 713–715. https://doi.org/10.1016/j.atmosenv.2013.09.034

Wei, J., Peng, Y., Mahmood, R., Sun, L., & Guo, J. (2019). Intercomparison in spatial distributions and temporal trends derived from multi-source satellite aerosol products. *Atmospheric Chemistry and Physics*, *19*(10), 7183–7207. https://doi.org/10.5194/acp-19-7183-2019

Xu, X., Wang, J., Wang, Y., Zeng, J., Torres, O., Reid, J. S., et al. (2019). Detecting layer height of smoke aerosols over vegetated land and water surfaces via oxygen absorption bands: Hourly results from EPIC/DSCOVR in deep space. *Atmospheric Measurement Techniques*, *12*(6), 3269–3288. https://doi.org/10.5194/amt-12-3269-2019

Zhang, Y., Li, Y., Guo, J., Wang, Y., Chen, D., & Chen, H. (2019). The climatology and trend of black carbon in China from 12-year ground observations. *Climate Dynamics*, *53*(9–10), 5881–5892. https://doi.org/10.1007/s00382-019-04903-0